Geophysical Research Letters

RESEARCH LETTER
10.1029/2025GL119720

Large Uncertainty in Arctic Warming Driven by the Atlantic Meridional Overturning Circulation

L. C. Hahn[1], I. Eisenman[1], N. J. Lutsko[1], V. Meccia[2], O. Mehling[3], and K. Bellomo[4]

[1]Scripps Institution of Oceanography, UC San Diego, San Diego, CA, USA, [2]National Research Council, Institute of Atmospheric Sciences and Climate, Bologna, Italy, [3]Institute for Marine and Atmospheric Research, Utrecht University, Utrecht, The Netherlands, [4]Department of Geosciences, Università di Padova, Padova, Italy

Key Points:

- Intermodel spread in the AMOC decline, imposed in a single model, reproduces nearly half the total intermodel spread in Arctic warming
- A smaller AMOC decline increases Arctic warming via increased ocean heat transport, latent heat transport, and positive local feedbacks
- Changes in sea-ice area mediate the sensitivity of Arctic warming to the AMOC decline

Supporting Information:

Supporting Information may be found in the online version of this article.

Correspondence to:

L. C. Hahn,
lihahn@ucsd.edu

Citation:

Hahn, L. C., Eisenman, I., Lutsko, N. J., Meccia, V., Mehling, O., & Bellomo, K. (2025). Large uncertainty in Arctic warming driven by the Atlantic meridional overturning circulation. *Geophysical Research Letters*, *52*, e2025GL119720. https://doi.org/10.1029/2025GL119720

Received 30 SEP 2025
Accepted 24 NOV 2025

Abstract Climate models project a weakening of the Atlantic Meridional Overturning Circulation (AMOC) that will reduce Arctic warming. However, there is substantial intermodel spread in the projected AMOC decline, and its contribution to uncertainty in projected Arctic warming has not yet been quantified. To investigate this, we perform model experiments that increase CO_2 concentrations while imposing the intermodel spread in the AMOC decline. We find that this intermodel spread in the AMOC decline reproduces 45% of the total intermodel spread in Arctic warming. A smaller AMOC decline increases Arctic warming via increased northward ocean heat transport, atmospheric moisture transport, and positive Arctic feedbacks. Arctic warming is more sensitive to AMOC differences that produce larger sea-ice changes. Combined with a strong correlation between a small AMOC decline and Arctic warming across models, these results indicate that ocean circulation is a key source of model uncertainty in projections of Arctic warming.

Plain Language Summary The Arctic is warming faster than any other region on Earth in response to increased concentrations of greenhouse gases in the atmosphere. In climate model projections, Arctic warming is partly offset by a change in ocean circulation in the Atlantic that cools the Arctic. However, different climate models project widely different changes in this ocean circulation. Here we investigate how these model differences in ocean circulation contribute to model differences in Arctic warming. When we impose model differences in ocean circulation in a single model, we can reproduce almost half of the total model spread in projected Arctic warming. The impact of ocean circulation on Arctic warming depends on sea ice changes; larger changes in sea-ice area enable larger changes in Arctic warming. Our results indicate that ocean circulation is a key source of uncertainty in model projections of Arctic warming.

1. Introduction

In climate model projections, the Arctic exhibits both the largest warming and the largest warming uncertainty of any region on Earth (e.g., L. C. Hahn et al., 2021; Holland & Bitz, 2003; IPCC, 2001; Manabe & Wetherald, 1975). Structural differences between models are the primary source of uncertainty in Arctic sea-ice and warming projections, larger than uncertainty due to emissions scenario or internal variability (Bonan et al., 2021; Lehner et al., 2020; Notz & SIMIP Community, 2020). Previous studies have used offline energy budget diagnostics to investigate the sources of this model uncertainty, including the roles of radiative forcing, climate feedbacks, atmospheric heat transport, and ocean heat uptake. These studies find that model uncertainty in Arctic warming is primarily driven by the albedo feedback and its positive covariance with the lapse-rate feedback, with a small or nonexistent role for changes in ocean heat uptake (Block et al., 2020; L. C. Hahn et al., 2021; Pithan & Mauritsen, 2014). However, such diagnostic approaches are limited by their implicit inclusion of interactions between different mechanisms, which may obscure the underlying drivers of uncertainty in Arctic warming. In particular, other studies suggest an important role for ocean heat transport, finding positive correlations between poleward ocean heat transport and Arctic sea-ice loss and warming across climate models (Aylmer et al., 2024; Holland & Bitz, 2003; Hwang et al., 2011; Mahlstein & Knutti, 2011; Nummelin et al., 2017; Pan et al., 2023).

Here we investigate a potential underlying source of uncertainty in ocean heat transport and Arctic warming—the Atlantic Meridional Overturning Circulation (AMOC). Climate models consistently project a weakening of this ocean circulation in a warming world (Fox-Kemper et al., 2021; Weijer et al., 2020). Projected AMOC weakening has been shown to significantly reduce Arctic warming by reducing northward ocean heat transport, ocean-to-atmosphere heating, and positive Arctic feedbacks, particularly the albedo feedback (He et al., 2017; Lee

10.1029/2025GL119720

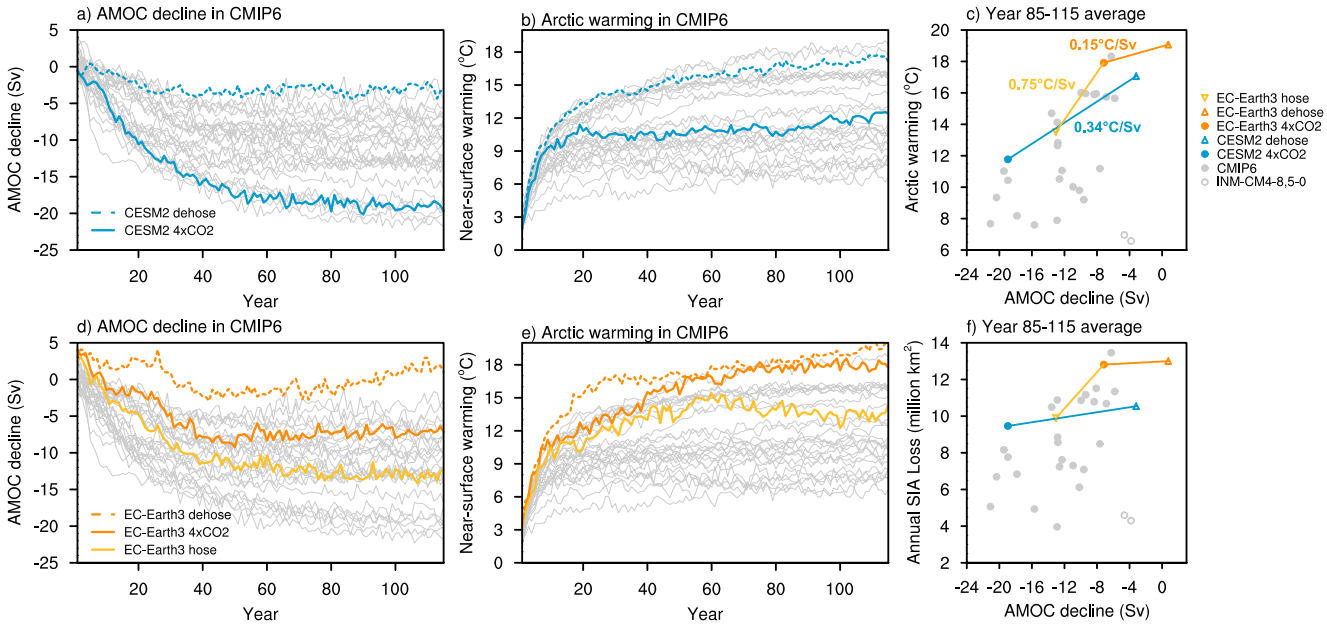

Figure 1. Intermodel spread across 28 CMIP6 models (grey lines) in (a, d) the AMOC decline (Sv) and (b, e) Arctic near-surface warming (°C; north of 60°N) for an abrupt CO_2 quadrupling experiment (*4xCO2*) compared to a preindustrial control experiment. The AMOC strength is calculated as the maximum in the ocean meridional overturning mass streamfunction in the Atlantic north of 30°N and at depth greater than 500 m (e.g., Liu et al., 2020). The CESM2 *4xCO2* and *dehose* experiments are overlaid in blue in panels (a, b), and the EC-Earth3 *4xCO2, dehose*, and *hose* experiments are overlaid in orange in panels (d, e). Averages over years 85–115 for all experiments are shown for the AMOC decline (Sv) vs. (c) Arctic warming (°C) and (f) Arctic sea-ice area loss (million km^2).

et al., 2024; Liu et al., 2020; Rugenstein et al., 2013). However, different climate models project widely different degrees of AMOC weakening. In the latest generation of models participating in the Coupled Model Intercomparison Project Phase 6 (CMIP6) under abrupt CO_2 quadrupling, the AMOC decline ranges from 17% to 82% of its preindustrial strength (Figure 1a, grey lines; Bellomo et al., 2021; L. C. Hahn et al., 2025). Models with a smaller AMOC decline tend to produce greater Arctic warming (Figure 1c, grey dots; $r^2 = 0.45$, $p < 0.001$, excluding the outliers INM-CM4-8, 5-0). Combined with studies like Rugenstein et al. (2013) that demonstrate the influence of the AMOC on Arctic warming, this correlation suggests that model uncertainty in the AMOC decline may contribute significant uncertainty in Arctic warming. However, many other factors influence Arctic warming in these comprehensive experiments, making it difficult to establish causality from these correlations alone. The impact of uncertainty in the AMOC decline on uncertainty in Arctic warming has not yet been quantified.

To investigate how uncertainty in the AMOC decline impacts Arctic warming, we perform new experiments that impose the CMIP6 range in AMOC declines within the CESM2 climate model. We perform similar experiments in the EC-Earth3 model to evaluate how robust these mechanisms are across models and to investigate how sea ice mediates the Arctic warming sensitivity to AMOC uncertainty. We quantify the effects of the AMOC on Arctic warming through changes to ocean heat uptake, atmospheric heat and moisture transport, and climate feedbacks. Using targeted model experiments, this study highlights an overlooked source of uncertainty in previous diagnostic analyses: the role of the AMOC decline.

2. Methods

2.1. CESM2 and EC-Earth3 Experiments

To explore the impact of AMOC uncertainty on Arctic warming, we use idealized experiments in the fully-coupled Community Earth System Model Version 2 (CESM2) at a nominal 1° horizontal resolution (Danabasoglu et al., 2020). This model includes the Community Atmosphere Model Version 6 (CAM6), the Parallel Ocean Program Version 2 (POP2; Smith et al., 2010), and the Los Alamos Sea Ice Model Version 5.1.2 (CICE5; Hunke et al., 2015). In addition to CESM2, we use the EC-Earth3 model at a nominal 1° ocean resolution and ~80 km atmospheric resolution (Döscher et al., 2022). EC-Earth3 includes the Integrated Forecast System (IFS) CY36R4 atmosphere model, the NEMO3.6 ocean model (Madec, 2015), and the LIM3 sea-ice model (Rousset et al., 2015).

In addition to standard abrupt CO_2 quadrupling experiments (*abrupt-4xCO2,* abbreviated here as *4xCO2*; Eyring et al., 2016), we perform new experiments in CESM2 and EC-Earth3 that abruptly quadruple CO_2 while perturbing the surface freshwater budget to control the AMOC strength. These experiments add or remove surface freshwater through a virtual salinity flux in the Arctic and in the North Atlantic north of 50°N, with a compensating salinity flux elsewhere to conserve the global ocean salt content. This freshwater forcing follows the North Atlantic Hosing Model Intercomparison Project protocol (NAHosMIP; Jackson et al., 2023).

The CESM2 *4xCO2* experiment has one of the largest AMOC declines across CMIP6 models (solid blue line, Figure 1a). In contrast, the CESM2 *dehose* experiment applies a constant −0.5 Sv freshwater flux via a virtual salinity flux to reproduce the smallest AMOC decline seen in CMIP6 (dashed blue line, Figure 1a). By comparing the *dehose* and *4xCO2* experiments, we can therefore assess how the CMIP6 spread in the AMOC decline, imposed in a single model, impacts Arctic warming. We note that these CESM2 experiments span most, but not all, of the CMIP6 spread in the AMOC decline (Figure 1a); imposing the full spread may produce a larger impact on warming. We run the *dehose* experiment for 115 years rather than the standard 150-year period to conserve computing resources, as the CMIP6 spread in the AMOC decline at year 115 captures most of the spread at year 150. The magnitude and pattern of ocean heat uptake anomalies associated with AMOC differences in our CESM2 experiments is similar to that across CMIP6 models (L. C. Hahn et al., 2025), suggesting that these experiments in a single model are useful for understanding the impact of AMOC spread across CMIP6.

In contrast to CESM2, the standard EC-Earth3 *4xCO2* experiment has one of the smallest AMOC declines across CMIP6 (solid orange line, Figure 1d). We compare this with the EC-Earth3 *dehose* experiment developed by Bellomo and Mehling (2024), which applies a −0.4 Sv freshwater flux under CO_2 quadrupling to produce a near-zero AMOC decline (dashed orange line, Figure 1d). In addition, we perform the EC-Earth3 *hose* experiment (yellow line, Figure 1d), which applies a +0.3 Sv freshwater flux under CO_2 quadrupling to produce a larger AMOC decline than EC-Earth3 *4xCO2*. Combined with experiments in CESM2, these EC-Earth3 experiments allow us to explore the sensitivity of our results to model choice and to investigate how sea ice influences the Arctic warming sensitivity to uncertainty in the AMOC decline. We do not have a CESM2 *hose* experiment because the AMOC is already so weak in CESM2 *4xCO2* (Figure S1b in Supporting Information S1) that we are unable to weaken it further with additional hosing. This AMOC resilience to further weakening may result from Southern Ocean wind-driven upwelling that must be balanced by downwelling in the Atlantic or Pacific (Baker et al., 2025).

2.2. Warming Contribution Methodology

To understand how uncertainty in the AMOC decline impacts Arctic warming, we calculate contributions to Arctic warming from changes in ocean heat uptake, atmospheric heat transport, and climate feedbacks. Following previous studies (Crook & Forster, 2011; Feldl & Roe, 2013; Goosse et al., 2018; L. C. Hahn et al., 2021; Lu & Cai, 2009; Pithan & Mauritsen, 2014; Taylor et al., 2013), we use a local energy budget analysis to calculate these warming contributions. In light of substantial long-term variability in the AMOC in the EC-Earth3 preindustrial control (*piControl*) experiment (Figure S1a in Supporting Information S1; Meccia et al., 2023; Mehling et al., 2024), we calculate anomalies for CO_2 quadrupling experiments (the *4xCO2*, *dehose*, and *hose* experiments) compared to a 150-year average of the corresponding *piControl* experiment. We calculate warming contributions using anomalies averaged over years 85–115 after CO_2 quadrupling and quantify climate feedbacks using the quotient of anomalies in top-of-atmosphere (TOA) radiation and near-surface temperature averaged over this period.

We decompose the net climate feedback into the albedo, Planck, lapse-rate, water vapor, and cloud feedbacks using the radiative kernel method described in Shell et al. (2008) and Soden et al. (2008). We use radiative kernels derived from the ERA-Interim reanalysis by Huang et al. (2017), which yield the smallest feedback residual compared to other radiative kernels in CMIP6 *4xCO2* experiments (Zelinka et al., 2020). We calculate the total atmospheric heat transport (AHT) convergence as the difference between surface and net TOA fluxes (e.g., Pithan & Mauritsen, 2014). We partition this further into moist AHT convergence, calculated as the difference between precipitation and evaporation multiplied by the latent heat of vaporization, and dry AHT convergence, calculated as the residual between the total and moist AHT convergence (e.g., L. C. Hahn et al., 2021; Kay et al., 2012). The ocean heat uptake term is calculated using surface heat fluxes (positive into the atmospheric column) which include both ocean heat transport and ocean heat storage.

Using a local energy budget (Equation 1), we can convert these energetic contributions of climate feedbacks ($\lambda_i \Delta T$), the Planck response ($\lambda_p \Delta T$), and anomalies in AHT convergence (ΔAHT) and ocean heat uptake (ΔO) into contributions to near-surface Arctic warming (ΔT) in years 85–115 for each CO_2 quadrupling experiment compared to the *piControl* experiment. Here and throughout this study, the Arctic is defined as the region from 60 to 90°N. Equation 1 also includes the radiative forcing (F) and a residual term (ΔR_{res}):

$$F + \left(\lambda_p + \sum\nolimits_i \lambda_i\right)\Delta T + \Delta AHT + \Delta O + \Delta R_{\text{res}} = 0 \tag{1}$$

Warming contributions are defined by dividing each term in Equation 1 (in W m^{-2}) by the strength of the Arctic Planck response in the *4xCO2* experiment ($\overline{\lambda_p}$, in W m^{-2} K^{-1}):

$$\Delta T = -\frac{F}{\overline{\lambda_p}} - \frac{\lambda_p' \Delta T}{\overline{\lambda_p}} - \frac{\sum_i \lambda_i \Delta T}{\overline{\lambda_p}} - \frac{\Delta AHT}{\overline{\lambda_p}} - \frac{\Delta O}{\overline{\lambda_p}} - \frac{\Delta R_{res}}{\overline{\lambda_p}} \tag{2}$$

where $\lambda_p' = \lambda_p - \overline{\lambda_p}$ is the difference between the Arctic Planck response (λ_p) in a given CO_2 quadrupling experiment and its value in the *4xCO2* experiment. Following Equation 2, we calculate contributions to Arctic warming in CESM2 *dehose−piControl* and CESM2 *4xCO2−piControl* before taking the difference between these sets of experiments. We assume there is a negligible warming contribution from forcing differences between CESM2 *dehose* and *4xCO2,* which have identical CO_2 concentrations. Similarly, we calculate contributions to Arctic warming in EC-Earth3 *dehose−piControl*, EC-Earth3 *hose−piControl*, and EC-Earth3 *4xCO2−piControl* before taking differences between these sets of experiments. As in CESM2, we assume a negligible contribution from forcing to warming differences between EC-Earth3 *dehose*, *hose*, and *4xCO2*.

3. Results

A smaller AMOC decline in CESM2 *dehose* than *4xCO2* increases Arctic warming by 5.3°C, a 45% increase from the *4xCO2* experiment, averaged over years 85–115 after CO_2 quadrupling (blue lines, Figure 1b; blue markers, Figure 1c). This is also about 45% of the total intermodel spread in Arctic warming across CMIP6 models. In other words, the intermodel spread in the AMOC decline, imposed in a single model, can reproduce almost half the total intermodel spread in Arctic warming. A smaller AMOC decline increases surface warming most prominently in the subpolar North Atlantic, collocated with the largest increase in ocean-to-atmosphere heating (Figure S2a and S2d in Supporting Information S1). Supported by an increase in poleward ocean heat transport (Figure S3a in Supporting Information S1), ocean-to-atmosphere heating is the primary driver of increased Arctic warming in *dehose−4xCO2* (Figure 2a). Positive local feedbacks further amplify warming with a smaller AMOC decline. This includes enhanced warming contributions from the albedo, water vapor, lapse-rate, and shortwave cloud feedbacks, consistent with previous analyses of idealized AMOC experiments (Lee et al., 2024).

The lapse-rate and shortwave cloud feedbacks become more-positive particularly in the subpolar North Atlantic (Figure S4c and S4d in Supporting Information S1) as a result of increased northward ocean heat transport that reduces the lower tropospheric stability and low-cloud cover (L. C. Hahn et al., 2025). Increased warming supports a more-positive water vapor contribution throughout the Arctic (Figure S4b in Supporting Information S1), and accelerated sea-ice loss supports a more-positive albedo contribution particularly to the north of 70°N in Baffin Bay, the Laptev Sea, and the central Arctic (Figure S4a and S2g in Supporting Information S1). Arctic warming is also amplified by an increase in poleward moist AHT and damped by a reduction in dry AHT (Figure 2a; Figure S3a in Supporting Information S1). Both are consistent with down-gradient diffusion of temperature and moisture anomalies: stronger meridional moisture gradients in the warmer climate of the *dehose* experiment increase poleward moist AHT, while dry AHT weakens in response to larger Arctic-amplified warming (e.g., Armour et al., 2019; Feldl et al., 2017; L. C. Hahn et al., 2021; Hwang et al., 2011; Pithan & Mauritsen, 2014; Roe et al., 2015).

As illustrated by this warming contribution analysis, increased sea-ice loss and a positive albedo feedback amplify the warming produced by a stronger AMOC in CESM2 *dehose* compared to *4xCO2* (Figure 2a; Figures 3a–3c). However, there is little sea ice by the end of the CESM2 *4xCO2* experiment, and sea-ice loss saturates with

10.1029/2025GL119720

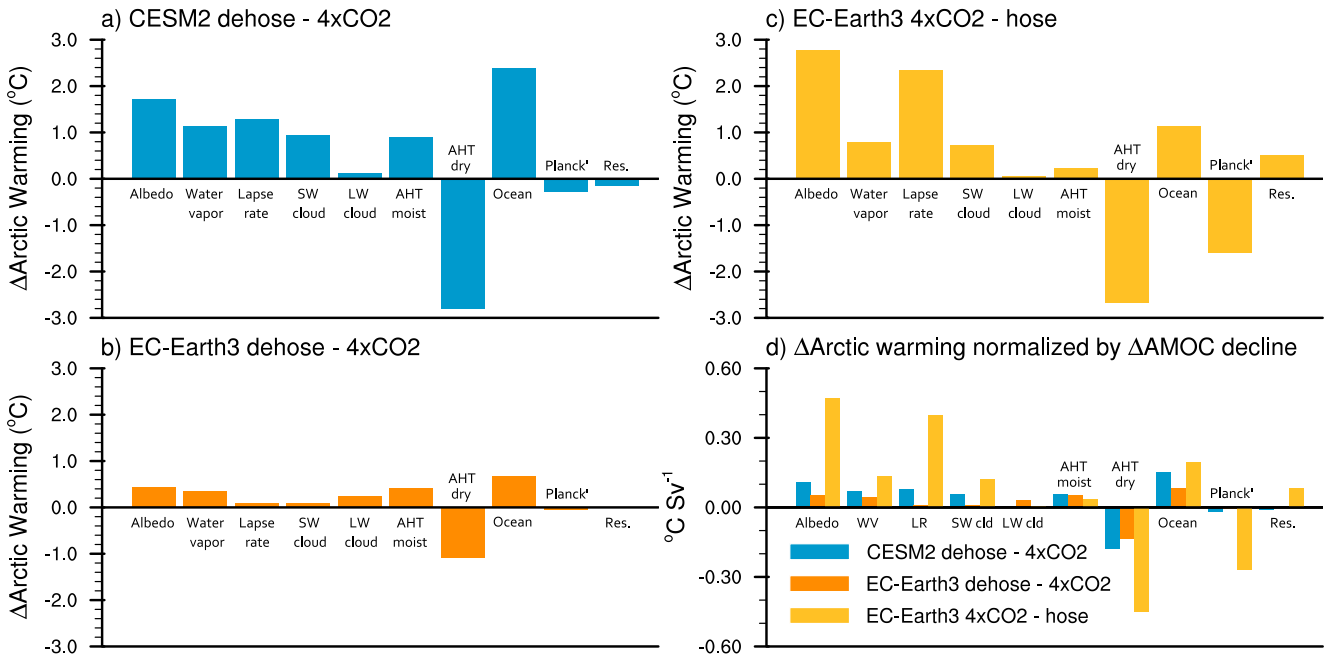

Figure 2. Contributions to Arctic warming differences (°C; north of 60°N) averaged over years 85–115 after abrupt CO_2 quadrupling for (a) CESM2 *dehose−4xCO2*, (b) EC-Earth3 *dehose−4xCO2*, (c) EC-Earth3 *4xCO2−hose*, and (d) all sets of experiments, normalized by each set's difference in the AMOC decline. Warming contributions are shown for the surface albedo, water vapor, lapse-rate, shortwave (SW) cloud, and longwave (LW) cloud feedbacks, the change in moist and dry atmospheric heat transport convergence (AHT moist; AHT dry) and ocean heat loss to the atmosphere (Ocean), the variation in the Planck response from its *4xCO2* value (Planck'), and a residual term (Res.).

additional warming in CESM2 *dehose* as the Arctic becomes ice-free. Does this saturation of sea-ice loss limit the increase in surface warming in CESM2 *dehose−4xCO2*? As a reminder, CESM2 *4xCO2* has a very large AMOC decline, and we span the intermodel spread in the AMOC decline by imposing a smaller AMOC decline in *dehose* (Figure 1a). If we instead use a model with a small AMOC decline in the standard *4xCO2* experiment and impose a larger AMOC decline, we would expect a relative sea-ice growth that is unsaturated and may therefore support a larger sensitivity of Arctic warming to AMOC uncertainty.

To test how sea ice mediates the sensitivity of Arctic warming to the AMOC decline, we use the EC-Earth3 model, which projects a small AMOC decline in the standard *4xCO2* experiment (solid orange line, Figure 1d). As in CESM2, we compare EC-Earth3 *4xCO2* with a *dehose* experiment that produces a smaller AMOC decline (dashed orange line, Figure 1d), but we additionally perform an EC-Earth3 *hose* experiment that produces a larger AMOC decline (yellow line, Figure 1d). A small AMOC decline in EC-Earth3 *4xCO2* supports one of the largest Arctic warming signals among the CMIP6 models (Figure 1e), and results in minimal sea-ice cover by the end of the EC-Earth3 *4xCO2* experiment (Figure 3d), even less than in CESM2 *4xCO2*. As found in CESM2, imposing a smaller AMOC decline in EC-Earth3 *dehose* versus EC-Earth3 *4xCO2* increases northward ocean heat transport (Figure S3b in Supporting Information S1) and ocean-to-atmosphere heating in the Arctic (Figure 2b; Figure S2e in Supporting Information S1). This allows for faster Arctic warming in the first 30 years of EC-Earth3 *dehose* compared to *4xCO2* (dashed vs. solid orange lines, Figure 1e). However, the last 30 years of EC-Earth3 *dehose* show only a small increase in warming compared to *4xCO2* (compare dashed and solid orange lines in Figure 1e). This small warming sensitivity in years 85–115 results from a small difference in sea ice: with minimal sea-ice in the EC-Earth3 *4xCO2* experiment (Figure 3d), additional warming in *dehose* produces an ice-free Arctic (Figure 3e) and limits sea-ice loss for *dehose−4xCO2* (Figure 3f). The existence of even less sea ice in EC-Earth3 *4xCO2* than in CESM2 *4xCO2* provides even less room for additional sea-ice loss in the *dehose* experiment. To a greater degree than in CESM2, the saturation of sea-ice loss limits the increase in warming in EC-Earth3 *dehose* versus *4xCO2*.

In contrast, imposing a larger AMOC decline in EC-Earth3 *hose* versus *4xCO2* has a much larger impact on surface warming than the *dehose* experiment in years 85–115 (Figure 1e). A larger AMOC decline in EC-Earth3

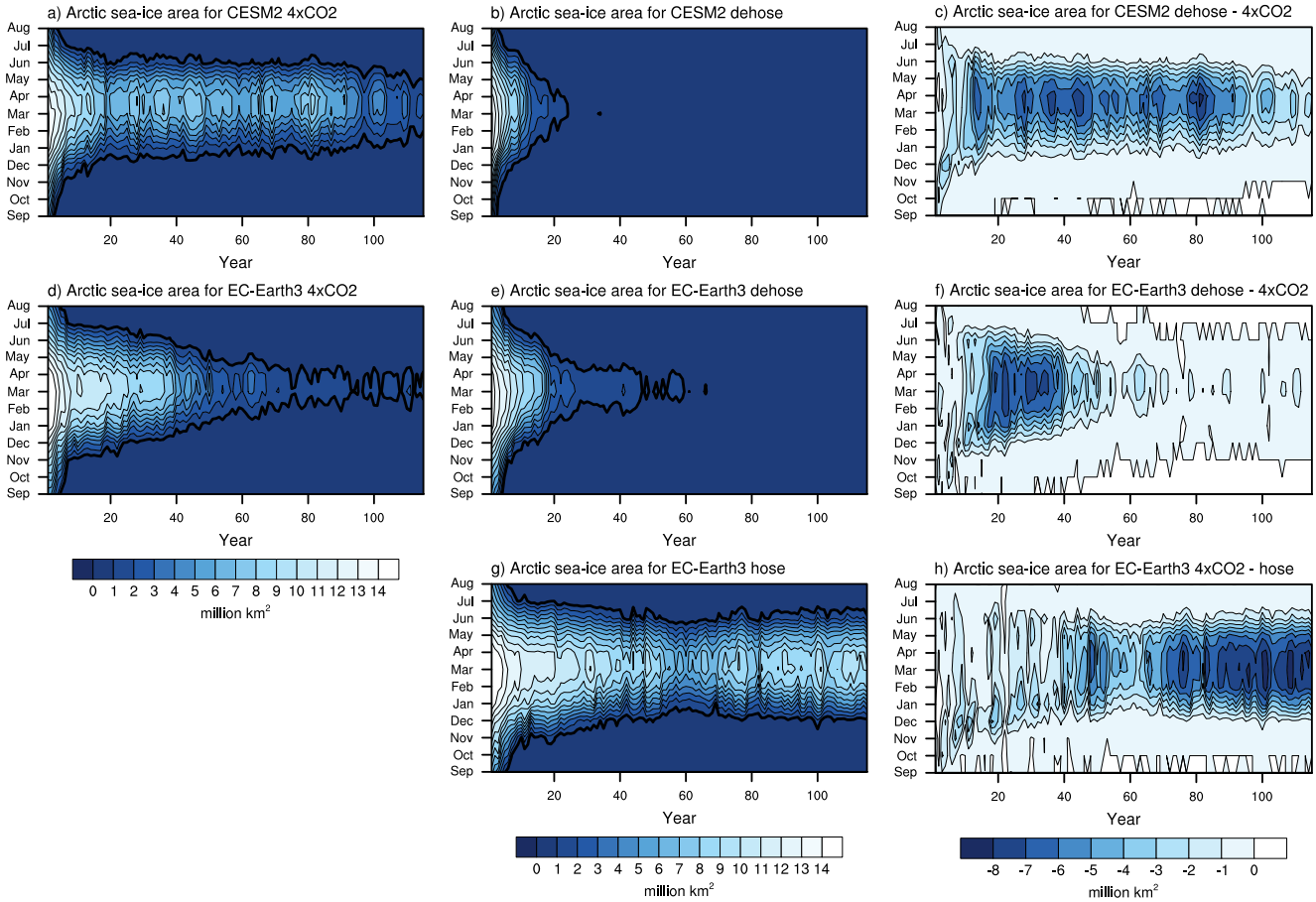

Figure 3. Monthly Arctic sea-ice area (million km^2) in year 1–115 for (a) CESM2 *4xCO2*, (b) CESM2 *dehose*, (c) CESM2 *dehose−4xCO2*, (d) EC-Earth3 *4xCO2*, (e) EC-Earth3 *dehose*, (f) EC-Earth3 *dehose−4xCO2*, (g) EC-Earth3 *hose*, and (h) EC-Earth3 *4xCO2−hose* experiments. The bold contour (a, b, d, e, g) indicates a sea-ice area of 1 million km^2.

hose sustains a greater sea-ice area than in *4xCO2* in years 85–115 (Figure 3g). This produces a large, unsaturated difference in sea-ice area for EC-Earth3 *4xCO2−hose* (Figure 3h), larger than for EC-Earth3 *dehose−4xCO2* or CESM2 *dehose−4xCO2*. A larger difference in sea-ice area supports a higher sensitivity of Arctic warming to AMOC differences in EC-Earth3 *4xCO2−hose* (0.75°C/Sv) than in EC-Earth3 *dehose−4xCO2* (0.15°C/Sv) or CESM2 *dehose−4xCO2* (0.34°C/Sv), as illustrated in Figures 1c and 1f (yellow lines vs. orange and blue lines). In other words, Arctic warming is more than twice as sensitive to AMOC perturbations when the perturbation preserves sea ice (i.e., induces a relative sea-ice recovery compared to *4xCO2*) in the EC-Earth3 hosing experiment, than when it accelerates sea-ice loss in the CESM2 dehosing experiment.

To confirm that these differences in warming sensitivity are driven by differences in sea ice, we compare contributions to warming in EC-Earth3 *4xCO2−hose* with the *dehose−4xCO2* experiments in EC-Earth3 and CESM2. As in the *dehose−4xCO2* experiments, a smaller AMOC decline in EC-Earth3 *4xCO2 − hose* amplifies Arctic warming via increased ocean-to-atmosphere heating and positive Arctic feedbacks (Figure 2c). A more-negative Planck feedback in *4xCO2* compared to *hose* results from a larger ratio of surface to near-surface warming, particularly over high-latitude land (not shown). We normalize these warming contributions by the difference in AMOC decline in each set of experiments to better compare them (Figure 2d). These normalized warming contributions illustrate that the dominant contributors to higher warming sensitivity in the hosing experiment are the albedo and lapse-rate feedbacks, consistent with a key role for sea ice in mediating Arctic warming sensitivity to the AMOC decline. Larger changes in sea ice produce not only a stronger albedo feedback but also a more-positive lapse-rate feedback by supporting surface-amplified temperature changes (Boeke et al., 2021; Feldl et al., 2017, 2020; Graversen et al., 2014). When we impose a smaller AMOC decline in the *dehose* experiments, sea-ice loss saturates and limits changes in the surface albedo and lapse rate, limiting the resulting

increase in warming. Instead, when we impose a larger AMOC decline in the *hose* experiment, a relative sea-ice recovery compared to *4xCO2* substantially weakens the albedo and lapse-rate feedbacks and reduces surface warming.

The spatial structure of Arctic warming further illustrates the role of sea ice for the warming sensitivity to AMOC differences. In CESM2 and EC-Earth3 *dehose−4xCO2*, which have small sea-ice changes and Arctic warming sensitivity, the largest increase in warming occurs in the subpolar North Atlantic (Figure S2a and S2b in Supporting Information S1), collocated with the largest increase in ocean-to-atmosphere heating (Figure S2d and S2e in Supporting Information S1). In contrast, the largest increase in warming in the more sensitive EC-Earth3 *4xCO2−hose* experiments occurs in the Beaufort Sea and central Arctic, supported by a collocated reduction in sea-ice area (Figure S2c and S2i in Supporting Information S1) that produces more-positive albedo and lapse-rate feedbacks (Figure S6a and S6c in Supporting Information S1). These collocated maxima in sea-ice loss, sea-ice feedbacks, and increased Arctic warming in EC-Earth3 *4xCO2−hose* again indicate the key role of sea ice for amplifying the warming sensitivity to AMOC differences.

4. Conclusions

We investigate the impact of model uncertainty in the AMOC decline on uncertainty in Arctic warming using idealized experiments with the CESM2 and EC-Earth3 models. Imposing the CMIP6 spread in the AMOC decline using CESM2 reproduces 45% of the total intermodel spread in Arctic warming. The EC-Earth3 *dehose−hose* experiments, which span a slightly smaller AMOC difference (13.8 Sv) than CESM2 *dehose−4xCO2* (15.8 Sv), similarly reproduce 47% of the total intermodel spread in Arctic warming. A smaller AMOC decline allows for larger Arctic warming primarily by producing greater ocean-to-atmosphere heating. Warming is further amplified by poleward atmospheric moisture transport and positive local feedbacks, particularly the albedo feedback. The sensitivity of Arctic warming to the AMOC decline is strongly mediated by sea ice. Sea-ice loss saturates in experiments that impose a smaller AMOC decline, limiting the Arctic warming sensitivity to AMOC uncertainty; in experiments that impose a larger AMOC decline, unsaturated sea-ice growth and associated albedo and lapse-rate feedbacks support a larger sensitivity of Arctic warming to AMOC uncertainty.

Our results highlight the state-dependence of Arctic warming on the existence of sea ice, consistent with previous studies (e.g., Bellomo & Mehling, 2024; Holland & Landrum, 2021; Zhou et al., 2023). Bellomo and Mehling (2024) show that removing an AMOC decline by dehosing a *4xCO2* experiment impacts Arctic warming much less than imposing an AMOC decline by hosing a *piControl* experiment, presumably due to saturated sea-ice loss in the *4xCO2* experiment. By quantifying feedbacks in our experiments, we can confirm that state-dependent AMOC effects result from the saturation of sea-ice loss and positive albedo and lapse-rate feedbacks. Many studies have used hosing experiments under preindustrial conditions (e.g., NAHosMIP; Jackson et al., 2023) to understand the impacts of future AMOC weakening; our results suggest that dehosing experiments under increased CO_2 forcing are more applicable to investigate these state-dependent effects.

Combined with a strong correlation between a small AMOC decline and Arctic warming across CMIP6 models, our experiments indicate that the AMOC is an important source of uncertainty in projections of Arctic warming. A key implication is that intermodel spread in Arctic warming may be reduced by constraining the AMOC decline. Observational constraints based on the present-day strength of the AMOC (Weijer et al., 2020) and its return pathways (Baker et al., 2023) may substantially reduce uncertainty in the AMOC decline. Recent constraints predict a smaller AMOC decline than found in most model projections (Bonan et al., 2025), which we would expect to support a relatively large Arctic warming. Such constraints on the AMOC decline may substantially alter Arctic warming projections, particularly in models with more sea ice to lose.

Our results also illustrate that interactions between ocean circulation and climate feedbacks complicate interpretations of diagnostic warming contributions. Diagnostic approaches indicate that the albedo and lapse-rate feedbacks are the dominant sources of model uncertainty in Arctic warming (Block et al., 2020; L. C. Hahn et al., 2021; Pithan & Mauritsen, 2014). However, we find that both of these feedbacks are sensitive to underlying uncertainty in the AMOC decline. Idealized model experiments are needed to disentangle these interactions and understand underlying sources of uncertainty in Arctic warming. In addition to its impacts on Arctic feedbacks, the AMOC may impact Arctic warming by changing feedbacks beyond the Arctic (L. C. Hahn et al., 2025; He et al., 2017; Lin et al., 2019; Trossman et al., 2016; Zhang et al., 2010). In particular, a smaller AMOC decline allows for a more-positive shortwave cloud feedback in the North Atlantic midlatitudes. This may increase Arctic

warming by increasing poleward atmospheric heat transport, with warming further amplified by local Arctic feedbacks. Our diagnosed Arctic feedback contributions are impacted by both local and remote drivers; the relative role of each for the Arctic response to the AMOC decline remains an open question.

A caveat of this study is that different models may have different sensitivities of climate feedbacks and heat transports to the AMOC decline, producing different levels of Arctic warming sensitivity to an imposed AMOC perturbation. In particular, CESM2 simulates insufficient present and future sea-ice cover (Kay et al., 2022); imposing a small AMOC decline in models with more sea ice may support a larger sea-ice loss and Arctic warming. However, previous studies have found qualitatively similar impacts of the AMOC decline on ocean heat uptake, surface albedo, and Arctic warming in an earlier version of CESM (Lee et al., 2024; Liu et al., 2020) and in GFDL models (He et al., 2017; Rugenstein et al., 2013). Future work should assess the impact of AMOC constraints on Arctic warming across different climate models. In addition, while we investigate the impact of the AMOC on Arctic warming, on multi-decadal timescales Arctic warming and associated sea-ice melt can also impact the AMOC strength (e.g., Liu et al., 2019; Liu & Fedorov, 2022; Madan et al., 2024; Sévellec et al., 2017). These two-way interactions may further affect the relationship between uncertainty in the AMOC decline and uncertainty in Arctic warming.

Lastly, our experiments with different AMOC declines do not explore the influence of the preindustrial mean-state AMOC. In reality, models with a smaller AMOC decline tend to have a weaker mean-state AMOC strength (Bonan et al., 2025; Gregory et al., 2005; Jackson et al., 2020; Lin et al., 2023; Weaver et al., 2012; Weijer et al., 2020; Winton et al., 2014). We have shown that a model with a smaller AMOC decline supports larger Arctic warming by enhancing poleward ocean heat transport and sea-ice loss. A weaker mean-state AMOC in such a model may support additional Arctic warming by increasing the climatological Arctic sea-ice area and allowing for larger sea-ice loss in a warming climate. This positive correlation between climatological sea-ice area and Arctic warming has been shown in previous generations of climate models (Holland & Bitz, 2003; Rind et al., 1995) and also holds in CMIP6 models with saturated *4xCO2* sea-ice loss (Figure S7 in Supporting Information S1, black dots). Thus, mean-state AMOC uncertainty may amplify the effects of correlated uncertainty in the AMOC decline. Future work should isolate these potential impacts of model differences in the mean-state AMOC.

Conflict of Interest

The authors declare no conflicts of interest relevant to this study.

Data Availability Statement

Output from the *piControl* and *abrupt-4xCO2* experiments in CESM2 and other CMIP6 models can be found in the Earth System Grid Federation (ESGF) repository at https://esgf-node.llnl.gov/projects/esgf-llnl/. Model output from the CESM2 *dehose* experiment and the EC-Earth3 *dehose* and *hose* experiments is publicly available (L. Hahn, 2024; L. Hahn et al., 2025).

Acknowledgments
We thank Aixue Hu for sharing source code modifications to implement freshwater forcing in CESM2. L.C.H. was supported by the NOAA Climate and Global Change Postdoctoral Fellowship Program, administered by UCAR's Cooperative Programs for the Advancement of Earth System Science (CPAESS) under award #NA21OAR4310383 and #NA23OAR4310383B. N.J.L. was funded by NSF Grant OCE-2023520. I.E. was supported by NSF Grant OCE-2048590. K.B. was supported by the "The Geosciences for Sustainable Development" project (Budget Ministero dell'Università e della Ricerca–Dipartimenti di Eccellenza 2023–2027—C93C23002690001).

References

Armour, K. C., Siler, N., Donohoe, A., & Roe, G. H. (2019). Meridional atmospheric heat transport constrained by energetics and mediated by large-scale diffusion. *Journal of Climate*, *32*(12), 3655–3680. https://doi.org/10.1175/JCLI-D-18-0563.1

Aylmer, J. R., Ferreira, D., & Feltham, D. L. (2024). Impact of ocean heat transport on sea ice captured by a simple energy balance model. *Communications Earth & Environment*, *5*(1), 406. https://doi.org/10.1038/s43247-024-01565-7

Baker, J. A., Bell, M. J., Jackson, L. C., Renshaw, R., Vallis, G. K., Watson, A. J., & Wood, R. A. (2023). Overturning pathways control AMOC weakening in CMIP6 models. *Geophysical Research Letters*, *50*(14), e2023GL103381. https://doi.org/10.1029/2023GL103381

Baker, J. A., Bell, M. J., Jackson, L. C., Vallis, G. K., Watson, A. J., & Wood, R. A. (2025). Continued Atlantic overturning circulation even under climate extremes. *Nature*, *638*(8052), 987–994. https://doi.org/10.1038/s41586-024-08544-0

Bellomo, K., Angeloni, M., Corti, S., & von Hardenberg, J. (2021). Future climate change shaped by inter-model differences in Atlantic meridional overturning circulation response. *Nature Communications*, *12*(1), 3659. https://doi.org/10.1038/s41467-021-24015-w

Bellomo, K., & Mehling, O. (2024). Impacts and state-dependence of AMOC weakening in a warming climate. *Geophysical Research Letters*, *51*(10), e2023GL107624. https://doi.org/10.1029/2023GL107624

Block, K., Schneider, F. A., Mülmenstädt, J., Salzmann, M., & Quaas, J. (2020). Climate models disagree on the sign of total radiative feedback in the Arctic. *Tellus A: Dynamic Meteorology and Oceanography*, *72*(1), 1–14. https://doi.org/10.1080/16000870.2019.1696139

Boeke, R. C., Taylor, P. C., & Sejas, S. A. (2021). On the nature of the Arctic's positive lapse-rate feedback. *Geophysical Research Letters*, *48*, e2020GL091109. https://doi.org/10.1029/2020GL091109

Bonan, D. B., Lehner, F., & Holland, M. M. (2021). Partitioning uncertainty in projections of Arctic sea ice. *Environmental Research Letters*, *16*(4), 044002. https://doi.org/10.1088/1748-9326/abe0ec

Bonan, D. B., Thompson, A. F., Schneider, T., Zanna, L., Armour, K. C., & Sun, S. (2025). Observational constraints imply limited future Atlantic meridional overturning circulation weakening. *Nature Geoscience*, *18*(6), 479–487. https://doi.org/10.1038/s41561-025-01709-0

Crook, J. A., & Forster, P. M. (2011). A balance between radiative forcing and climate feedback in the modeled 20th century temperature response. *Journal of Geophysical Research*, *116*(D17), D17108. https://doi.org/10.1029/2011JD015924

Danabasoglu, G., Lamarque, J.-F., Bacmeister, J., Bailey, D. A., DuVivier, A. K., Edwards, J., et al. (2020). The Community Earth System Model Version 2 (CESM2). *Journal of Advances in Modeling Earth Systems*, *12*, e2019MS001916. https://doi.org/10.1029/2019MS001916

Döscher, R., Acosta, M., Alessandri, A., Anthoni, P., Arsouze, T., Bergman, T., et al. (2022). The EC-Earth3 Earth system model for the coupled model intercomparison project 6. *Geoscientific Model Development Discussions*, *15*(7), 2973–3020. https://doi.org/10.5194/gmd-15-2973-2022

Eyring, V., Bony, S., Meehl, G. A., Senior, C. A., Stevens, B., Stouffer, R. J., & Taylor, K. E. (2016). Overview of the Coupled Model Intercomparison Project Phase 6 (CMIP6) experimental design and organization. *Geoscientific Model Development*, *9*(5), 1937–1958. https://doi.org/10.5194/gmd-9-1937-2016

Feldl, N., Bordoni, S., & Merlis, T. M. (2017). Coupled high-latitude climate feedbacks and their impact on atmospheric heat transport. *Journal of Climate*, *30*(1), 189–201. https://doi.org/10.1175/JCLI-D-16-0324.1

Feldl, N., Po-Chedley, S., Singh, H. K. A., Hay, S., & Kushner, P. J. (2020). Sea ice and atmospheric circulation shape the high-latitude lapse rate feedback. *npj Climate and Atmospheric Science*, *3*(41), 41. https://doi.org/10.1038/s41612-020-00146-7

Feldl, N., & Roe, G. H. (2013). Four perspectives on climate feedbacks. *Geophysical Research Letters*, *40*(15), 4007–4011. https://doi.org/10.1002/grl.50711

Fox-Kemper, B., Hewitt, H. T., Xiao, C., Aðalgeirsdóttir, G., Drijfhout, S. S., Edwards, T. L., et al. (2021). Ocean, Cryosphere and Sea level change. In V. Masson-Delmotte, P. Zhai, A. Pirani, S. L. Connors, C. Péan, S. Berger, et al. (Eds.), *Climate change 2021: The physical science basis. Contribution of working group I to the sixth assessment report of the intergovernmental panel on climate change* (pp. 1211–1362). Cambridge University Press. https://doi.org/10.1017/9781009157896.011

Goosse, H., Kay, J. E., Armour, K. C., Bodas-Salcedo, A., Chepfer, H., Docquier, D., et al. (2018). Quantifying climate feedbacks in polar regions. *Nature Communications*, *9*(1), 1919. https://doi.org/10.1038/s41467-018-04173-0

Graversen, R. G., Langen, P. L., & Mauritsen, T. (2014). Polar amplification in CCSM4: Contributions from the lapse rate and surface Albedo feedbacks. *Journal of Climate*, *27*(12), 4433–4450. https://doi.org/10.1175/JCLI-D-13-00551.1

Gregory, J. M., & Coauthors. (2005). A model intercomparison of changes in the Atlantic thermohaline circulation in response to increasing atmospheric CO_2 concentration. *Geophysical Research Letters*, *32*, L12703. https://doi.org/10.1029/2005GL023209

Hahn, L. (2024). Supporting data for Hahn et al. J. Climate: Contribution of AMOC decline to uncertainty in global warming via ocean heat uptake and climate feedbacks [Dataset]. *Zenodo*. https://doi.org/10.5281/zenodo.14219338

Hahn, L., Meccia, V., Mehling, O., & Bellomo, K. (2025). Supporting data for Hahn et al. GRL: Large uncertainty in Arctic warming driven by the Atlantic Meridional Overturning Circulation [Dataset]. *Zenodo*. https://doi.org/10.5281/zenodo.17819750

Hahn, L. C., Armour, K. C., Zelinka, M. D., Bitz, C. M., & Donohoe, A. (2021). Contributions to polar amplification in CMIP5 and CMIP6 models. *Frontiers in Earth Science*, *9*, 710036. https://doi.org/10.3389/feart.2021.710036

Hahn, L. C., Lutsko, N. J., Eisenman, I., Luongo, M. T., & Xie, S.-P. (2025). Contribution of AMOC decline to uncertainty in global warming via Ocean heat uptake and climate feedbacks. *Journal of Climate*, *38*(21), 6245–6259. https://doi.org/10.1175/JCLI-D-24-0752.1

He, J., Winton, M., Vecchi, G., Jia, L., & Rugenstein, M. (2017). Transient climate sensitivity depends on base climate Ocean circulation. *Journal of Climate*, *30*(4), 1493–1504. https://doi.org/10.1175/JCLI-D-16-0581.1

Holland, M. M., & Bitz, C. M. (2003). Polar amplification of climate change in coupled models. *Climate Dynamics*, *21*(3–4), 221–232. https://doi.org/10.1007/s00382-003-0332-6

Holland, M. M., & Landrum, L. (2021). The emergence and transient nature of Arctic amplification in coupled climate models. *Frontiers of Earth Science*, *9*, 764. https://doi.org/10.3389/feart.2021.719024

Huang, Y., Xia, Y., & Tan, X. (2017). On the pattern of CO_2 radiative forcing and poleward energy transport. *Journal of Geophysical Research: Atmospheres*, *122*(20), 10578–10593. https://doi.org/10.1002/2017JD027221

Hunke, E. C., Lipscomb, W. H., Turner, A. K., Jeffery, N., & Elliott, S. (2015). *CICE: The Los Alamos Sea ice model. Documentation and software user's manual. Version 5.1*. T-3 Fluid Dynamics Group, Los Alamos National Laboratory, Tech. Rep. LA-CC-06-012.

Hwang, Y.-T., Frierson, D. M. W., & Kay, J. E. (2011). Coupling between Arctic feedbacks and changes in poleward energy transport. *Geophysical Research Letters*, *38*(17), L17704. https://doi.org/10.1029/2011GL048546

IPCC, Climate Change. (2001). In *The scientific basis. Contribution of Working Group 1 to the Third Assessment Report of the Intergovernmental Panel on Climate Change* J. T. Houghton, Y. Ding, D. J. Griggs, M. Noguer, P. J. van der Linden, et al. (Eds.), (p. 881). Cambridge University Press.

Jackson, L. C., Alastrué de Asenjo, E., Bellomo, K., Danabasoglu, G., Haak, H., Hu, A., et al. (2023). Understanding AMOC stability: The north Atlantic hosing model Intercomparison Project. *Geoscientific Model Development*, *16*(7), 1975–1995. https://doi.org/10.5194/gmd-16-1975-2023

Jackson, L. C., Roberts, M. J., Hewitt, H. T., Iovino, D., Koenigk, T., Meccia, V. L., et al. (2020). Impact of ocean resolution and mean state on the rate of AMOC weakening. *Climate Dynamics*, *55*(7–8), 1711–1732. https://doi.org/10.1007/s00382-020-05345-9

Kay, J. E., DeRepentigny, P., Holland, M. M., Bailey, D. A., DuVivier, A. K., Blanchard-Wrigglesworth, E., et al. (2022). Less surface sea ice melt in the CESM2 improves Arctic sea ice simulation with minimal non-polar climate impacts. *Journal of Advances in Modeling Earth Systems*, *14*(4), e2021MS002679. https://doi.org/10.1029/2021MS002679

Kay, J. E., Holland, M. M., Bitz, C. M., Blanchard-Wrigglesworth, E., Gettelman, A., Conley, A., & Bailey, D. (2012). The influence of local feedbacks and Northward heat transport on the equilibrium Arctic climate response to increased greenhouse gas forcing. *Journal of Climate*, *25*(16), 5433–5450. https://doi.org/10.1175/JCLI-D-11-00622.1

Lee, Y., Liu, W., Fedorov, A. V., Feldl, N., & Taylor, P. C. (2024). Impacts of Atlantic meridional overturning circulation weakening on Arctic amplification. *Proceedings of the national academy of sciences of the United States of America* (Vol. 121(39), p. e2402322121). https://doi.org/10.1073/pnas.2402322121

Lehner, F., Deser, C., Maher, N., Marotzke, J., Fischer, E. M., Brunner, L., et al. (2020). Partitioning climate projection uncertainty with multiple large ensembles and CMIP5/6. *Earth System Dynamics*, *11*(2), 491–508. https://doi.org/10.5194/esd-11-491-2020

Lin, Y., Rose, B. E. J., & Hwang, Y. (2023). Mean State AMOC affects AMOC weakening through subsurface warming in the Labrador Sea. *Journal of Climate*, *36*(12), 3895–3915. https://doi.org/10.1175/JCLI-D-22-0464.1

Lin, Y.-J., Hwang, Y.-T., Ceppi, P., & Gregory, J. M. (2019). Uncertainty in the evolution of climate feedback traced to the strength of the Atlantic meridional overturning circulation. *Geophysical Research Letters*, *46*(21), 12331–12339. https://doi.org/10.1029/2019GL083084

Liu, W., & Fedorov, A. (2022). Interaction between Arctic sea ice and the Atlantic meridional overturning circulation in a warming climate. *Climate Dynamics*, *58*(5–6), 1811–1827. https://doi.org/10.1007/s00382-021-05993-5

Liu, W., Fedorov, A., & Sévellec, F. (2019). The mechanisms of the Atlantic meridional overturning circulation slowdown induced by Arctic Sea ice decline. *Journal of Climate*, *32*, 977–996. https://doi.org/10.1175/JCLI-D-18-0231.1

Liu, W., Fedorov, A., Xie, S.-P., & Hu, S. (2020). Climate impacts of a weakened Atlantic meridional overturning circulation in a warming climate. *Science Advances*, *6*(26), eaaz4876. https://doi.org/10.1126/sciadv.aaz4876

Lu, J., & Cai, M. (2009). A new framework for isolating individual feedback processes in coupled general circulation climate models. Part I: Formulation. *Climate Dynamics*, *32*(6), 873–885. https://doi.org/10.1007/s00382-008-0425-3

Madan, G., Gjermundsen, A., Iversen, S. C., & LaCasce, J. H. (2024). The weakening AMOC under extreme climate change. *Climate Dynamics*, *62*(2), 1291–1309. https://doi.org/10.1007/s00382-023-06957-7

Madec, G. (2015). *NEMO ocean engine*. Note du Pole de modelisation de l'Institut Pierre-Simon Laplace No. 27.

Mahlstein, I., & Knutti, R. (2011). Ocean heat transport as a cause for model uncertainty in projected Arctic warming. *Journal of Climate*, *24*(5), 1451–1460. https://doi.org/10.1175/2010jcli3713.1

Manabe, S., & Wetherald, R. T. (1975). The effects of doubling the CO_2 concentration on the climate of a general circulation model. *Journal of the Atmospheric Sciences*, *32*(1), 3–15. https://doi.org/10.1175/1520-0469(1975)032<0003:TEODTC>2.0.CO;2

Meccia, V. L., Fuentes-Franco, R., Davini, P., Bellomo, K., Fabiano, F., Yang, S., & von Hardenberg, J. (2023). Internal multi-centennial variability of the Atlantic Meridional Overturning circulation simulated by EC-Earth3. *Climate Dynamics*, *60*(11–12), 3695–3712. https://doi.org/10.1007/s00382-022-06534-4

Mehling, O., Bellomo, K., & von Hardenberg, J. (2024). Centennial-scale variability of the Atlantic meridional overturning circulation in CMIP6 models shaped by Arctic–North Atlantic interactions and sea ice biases. *Geophysical Research Letters*, *51*(20), e2024GL110791. https://doi.org/10.1029/2024GL110791

Notz, D., & SIMIP Community. (2020). Arctic sea ice in CMIP6. *Geophysical Research Letters*, *47*(10), e2019GL086749. https://doi.org/10.1029/2019gl086749

Nummelin, A., Li, C., & Hezel, P. (2017). Connecting ocean heat transport changes from the midlatitudes to the Arctic Ocean. *Geophysical Research Letters*, *44*(4), 1899–1908. https://doi.org/10.1002/2016GL071333

Pan, R., Shu, Q., Wang, Q., Wang, S., Song, Z., He, Y., & Qiao, F. (2023). Future Arctic climate change in CMIP6 strikingly intensified by NEMO-family climate models. *Geophysical Research Letters*, *50*(4), e2022GL102077. https://doi.org/10.1029/2022GL102077

Pithan, F., & Mauritsen, T. (2014). Arctic amplification dominated by temperature feedbacks in contemporary climate models. *Nature Geoscience*, *7*(3), 181–184. https://doi.org/10.1038/ngeo2071

Rind, D., Healy, R., Parkinson, C., & Martinson, D. (1995). The role of sea ice in $2\times CO_2$ climate model sensitivity. Part I: The total influence of sea ice thickness and extent. *Journal of Climate*, *8*(3), 449–463. https://doi.org/10.1175/1520-0442(1995)008<0449:trosii>2.0.co;2

Roe, G., Feldl, N., Armour, K., Hwang, Y. T., & Frierson, D. M. W. (2015). The remote impacts of climate feedbacks on regional climate predictability. *Nature Geoscience*, *8*(2), 135–139. https://doi.org/10.1038/ngeo2346

Rousset, C., Vancoppenolle, M., Madec, G., Fichefet, T., Flavoni, S., Barthélemy, A., et al. (2015). The Louvain-la-Neuve sea ice model LIM3.6: Global and regional capabilities. *Geoscientific Model Development*, *8*(10), 2991–3005. https://doi.org/10.5194/gmd-8-2991-2015

Rugenstein, M. A. A., Winton, M., Stouffer, R. J., Griffies, S. M., & Hallberg, R. (2013). Northern high-latitude heat budget decomposition and transient warming. *Journal of Climate*, *26*(2), 609–621. https://doi.org/10.1175/JCLI-D-11-00695.1

Sévellec, F., Fedorov, A. V., & Liu, W. (2017). Arctic sea-ice decline weakens the Atlantic meridional overturning circulation. *Nature Climate Change*, *7*(8), 604–610. https://doi.org/10.1038/nclimate3353

Shell, K. M., Kiehl, J. T., & Shields, C. A. (2008). Using the radiative kernel technique to calculate climate feedbacks in NCAR's Community Atmospheric Model. *Journal of Climate*, *21*(10), 2269–2282. https://doi.org/10.1175/2007JCLI2044.1

Smith, R., & Coauthors. (2010). The Parallel Ocean Program (POP) reference manual, Ocean component of the Community Climate System Model (CCSM), LANL Tech. Report, LAUR-10-01853 (p. 141).

Soden, B. J., Held, I. M., Colman, R., Shell, K. M., Kiehl, J. T., & Shield, C. A. (2008). Quantifying climate feedbacks using radiative kernels. *Journal of Climate*, *21*(14), 3504–3520. https://doi.org/10.1175/2007JCLI2110.1

Taylor, P. C., Cai, M., Hu, A., Meehl, J., Washington, W., & Zhang, G. J. (2013). A decomposition of feedback contributions to polar warming amplification. *Journal of Climate*, *26*(18), 7023–7043. https://doi.org/10.1175/JCLI-D-12-00696.1

Trossman, D. S., Palter, J. B., Merlis, T. M., Huang, Y., & Xia, Y. (2016). Large-scale ocean circulation-cloud interactions reduce the pace of transient climate change. *Geophysical Research Letters*, *43*(8), 3935–3943. https://doi.org/10.1002/2016GL067931

Weaver, A. J., Sedláček, J., Eby, M., Alexander, K., Crespin, E., Fichefet, T., et al. (2012). Stability of the Atlantic meridional overturning circulation: A model intercomparison. *Geophysical Research Letters*, *39*(20), L20709. https://doi.org/10.1029/2012GL053763

Weijer, W., Cheng, W., Garuba, O. A., Hu, A., & Nadiga, B. T. (2020). CMIP6 models predict significant 21st century decline of the Atlantic Meridional Overturning Circulation. *Geophysical Research Letters*, *47*(12), e2019GL086075. https://doi.org/10.1029/2019GL086075

Winton, M., Anderson, W. G., Delworth, T. L., Griffies, S. M., Hurlin, W. J., & Rosati, A. (2014). Has coarse ocean resolution biased simulations of transient climate sensitivity? *Geophysical Research Letters*, *41*(23), 8522–8529. https://doi.org/10.1002/2014GL061523

Zelinka, M. D., Myers, T. A., McCoy, D. T., Po-Chedley, S., Caldwell, P. M., Ceppi, P., et al. (2020). Causes of higher climate sensitivity in CMIP6 models. *Geophysical Research Letters*, *47*(1), e2019GL0857. https://doi.org/10.1029/2019GL085782

Zhang, R., Kang, S. M., & Held, I. M. (2010). Sensitivity of climate change induced by the weakening of the Atlantic meridional overturning circulation to cloud feedback. *Journal of Climate*, *23*(2), 378–389. https://doi.org/10.1175/2009JCLI3118.1

Zhou, S.-N., Liang, Y.-C., Mitevski, I., & Polvani, L. M. (2023). Stronger Arctic amplification produced by decreasing, not increasing, CO_2 concentrations. *Environmental Research: Climate*, *2*(4), 045001. https://doi.org/10.1088/2752-5295/aceea2